NRC Research Press

ARTICLE

QCD test with the momentum spectra and the second binomial moment R_2 using e^+e^- data

M. Hasheminia, M.E. Zomorrodian, and A. Mirjalili

Abstract: Experimental data on the shape of hadronic momentum spectra are compared to the context of calculations in modified leading log approximation (MLLA), under the assumption of local parton hadron duality (LPHD). Considered are the inclusive momentum spectra and charged particle distributions in the reaction $e^+e^- \rightarrow$ hadrons, using the experimental as well as the Monte Carlo data at center of mass energies up to 200 GeV. Values of the second binomial moment R_2 obtained from the multiplicity distributions are also studied. Our results are compared with both experimental data from high and low energy e^+e^-, e^-p, and pp experiments and QCD calculations in various theoretical approaches. In general, good agreement is found between the measurements and the corresponding QCD predictions. A quantitative check of LPHD + MLLA has been performed by extracting a value of the strong coupling constant from the corresponding distributions. Possible explanations for all these features will be presented in this paper.

Key words: momentum spectra, second binomial moment, QCD models.

Résumé : Nous comparons les données expérimentales sur la forme des spectres d'impulsion hadronique aux résultats de calculs à l'ordre dominant de l'approximation log (MLLA) et en supposant une dualité locale parton hadron (LPHD). Nous considérons les spectres d'impulsion inclusive et les distributions de particules chargées dans les réactions $e^+e^- \rightarrow$ hadrons, utilisant les données expérimentales et les données Monte Carlo, dans des collisions à des énergies jusqu'à 200 GeV dans le centre de masse. Nous étudions aussi le second moment binomial expérimental R_2 obtenu à partir des distributions de multiplicité. Nous comparons nos résultats avec des données expérimentales de collisions e^+e^-, e^-p et pp de haute et basse énergie, ainsi qu'avec des résultats de calculs QCD de différentes approches. En général, un bon accord existe entre données expérimentales et résultats QCD. Nous procédons à une vérification quantitative de l'approche LPHD + MLLA en extrayant la valeur de la constante de couplage fort de la distribution correspondante. Ce papier présente une explication des caractéristiques observées. [Traduit par la Rédaction]

Mots-clés : spectre d'impulsion, second moment binomial, modèles QCD (CDQ).

1. Introduction

Hadron production in electron–positron annihilation plays an outstanding role in studying the dynamics of the strong interactions, described by the theory of quantum chromodynamics (QCD), [1]. Perturbative QCD can give quantitative analytical predictions based on the modified leading logarithmic approximation (MLLA) [2], under the assumption of local parton hadron duality (LPHD) [3].

The assumption of LPHD states that a calculated spectrum for partons in a parton shower can be related to the spectrum of real hadrons by simple normalization constants. The constants have to be determined by experiment. A second assumption is that the low momentum part of the spectrum is not influenced in a significant way by hadrons that are correlated to the primary quark.

Calculation of parton spectra in the MLLA takes into account next-to-leading logarithms in a consistent fashion. The physical mechanism relevant to these next-to-leading logarithms is the coherent emission of soft gluons inside a jet, leading to an angular ordering and an effective transverse momentum cutoff for the partons. Parton jets develop through repeated parton splitting, resulting in an increase of the multiplicity at lower momenta. The interplay of coherent emission of gluons and the creation of hadrons causes this spectrum to be cut off at very low momenta [1–3]. Calculations predict the shape of the distribution of $\xi = \ln(1/x_p)$ the so-called ξ spectrum, $x_p = (2p/\sqrt{s})$, where p and $\sqrt{s}$ are the momentum of the charged particles and the centre-of-mass (c.m.) energy, respectively. The resulting "hump-backed" distribution is nearly Gaussian.

In ref. 4 the low energy e^+e^- collision data has been analyzed for the momentum spectra, the multiplicity distribution, and the second binomial moment. We extend this analysis up to 200 GeV c.m. energies. The main reason behind this is to see if the features of the low energy data are also present in the high energy collisions, where we expect the non-perturbative effects to dominate. We do our measurements by using the AMY real data (based on e^+e^- annihilations at 60 GeV c.m. energy) as well as the Monte Carlo PYTHIA. We will compare our results with QCD calculations as well as those from high energy e^+e^-, ep, and $p\bar{p}$ and low energy (BES Collaboration) experiments.

2. Experimental setup

The central feature of the AMY detector is a 3 T solenoid magnet that allows the detector to be compact while maintaining good momentum resolution. Charged particles are detected efficiently

Received 19 September 2014. Accepted 20 June 2016.

M. Hasheminia and M.E. Zomorrodian. Department of Physics, Ferdowsi University of Mashhad, 91775-1436, Mashhad, Iran.
A. Mirjalili. Physics Department, University of Yazd, 89195-741 Yazd, Iran.
Corresponding author: M. Hasheminia (email: maryam.hasheminia@gmail.com).

Fig. 1. Distribution of $\xi = \ln(1/x_p)$ at several c.m. energies [7–15] compared to MLLA predictions in the limiting spectrum approach ([2], (2) in this paper) fitted to the data. The full lines indicate the region of the fit.

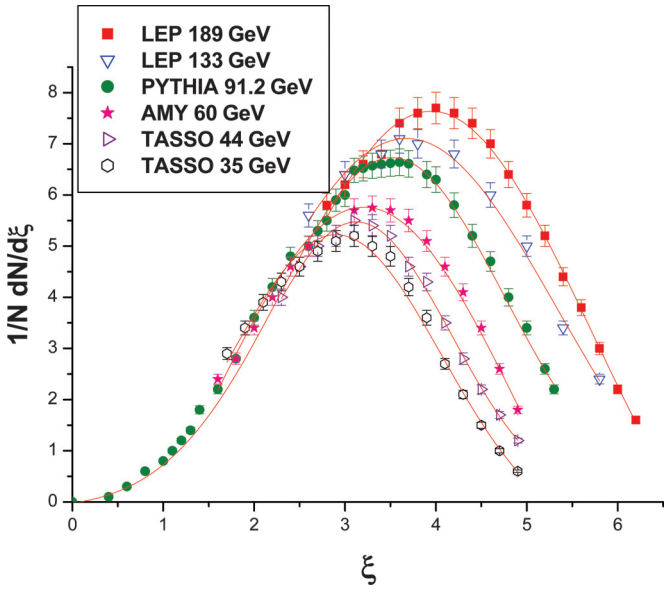

over the polar angle region $\cos\theta < 0.87$ with a momentum resolution $\Delta p_T = 0.7\% \times [p_T\ (\text{GeV/c})]$. The detailed description of various detector components has been given elsewhere [5].

3. ξ spectrum

A purely analytical approach giving quantitative predictions for ξ is a perturbative QCD calculation MLLA under the assumption of LPHD, expressed as [2]

$$\frac{1}{\sigma}\frac{d\sigma^h}{d\xi} = 2K^h\frac{C_F}{N_c}D^{\lim}(\xi, Y) \tag{1}$$

where $C_F = (N_c^2 - 1)/2N_c$ and K^h is a hadronization constant, which accounts for the number of hadrons of type h produced per final state parton. For the expression for the limiting spectrum distribution, $D^{\lim}(\xi, Y)$, we refer to ref. 2. In this formalism $Y = \ln(\sqrt{s}/2\Lambda_{eff})$, where Λ_{eff} is an effective scale factor representing both the QCD scale Λ and the cutoff scale Q_0. The MLLA limiting spectrum formalism predicts not only the shape of the ξ distribution, but apart from the hadronization correction, also predicts its normalization.

In Fig. 1 the measured ξ distribution is shown for our data along with the data obtained at both lower and higher energies [6–15], and compared with the fitted prediction of (1) where the free parameters are the effective scale Λ_{eff} and the hadronization constant K^h. We apply the formalism assuming three active flavors. The fit is also restricted around the peak. We find the peak describes the data well within the fitted range (full line). The data from the higher and lower energies follow the same trend as our data.

In Fig. 2 the obtained K^h factors are shown as a function of c.m. energy. Above 130 GeV the K^h factors are consistent with being constant. Below 50 GeV a modest rise in the values of K^h factors is observed. The high-order QCD theory predicts a rise in K^h factors, in particular at the lowest c.m. energies [3].

The position of the peak in the distribution is predicted to increase linearly with $Y = \ln(\sqrt{s}/2\Lambda_{eff})$. Corrections to this asymptotic

Fig. 2. The hadronization constant K^h at different $\sqrt{s}$ as obtained from the fit (see (2)) [7–15].

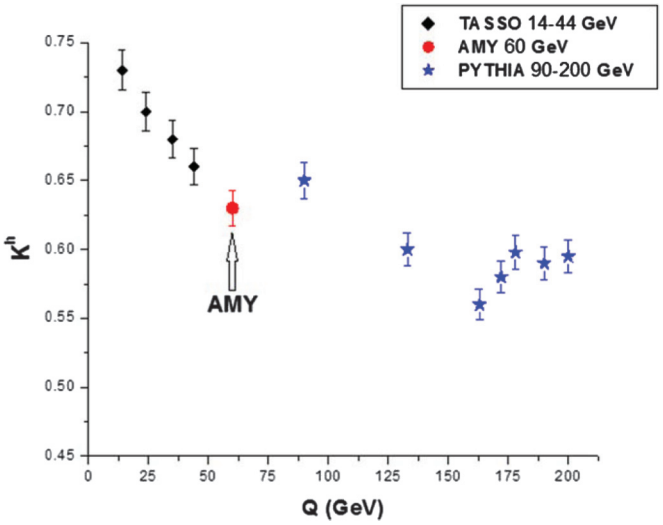

prediction were calculated up to $O(\alpha_s)$ by Fong and Webber [16] yielding a skewed Gaussian shape for the ξ spectrum

$$F_q(\xi, Y) = \frac{N(Y)}{\sigma\sqrt{2\pi}}\exp\left[\frac{k}{8} - \frac{s\delta}{2} - \frac{(2+k)\delta^2}{4} + \frac{s\delta^3}{6} + \frac{k\delta^4}{24}\right] \tag{2}$$

where $\delta = (\xi - \bar{\xi})/\sigma$ and, for quark initiated jets

$$\bar{\xi} = \frac{Y}{2}\left(1 + \frac{\rho}{24}\sqrt{\frac{48}{\beta Y}}\right)\left(1 - \frac{\omega}{6Y}\right) + \bar{\xi}_0 \tag{3}$$

$$\sigma = \sqrt{\frac{Y}{3}}\left(\frac{\beta Y}{48}\right)^{1/4}\left(1 - \frac{\beta}{64}\sqrt{\frac{48}{\beta Y}}\right)\left(1 + \frac{\omega}{8Y}\right) \tag{4}$$

$$s = -\frac{\rho}{16}\sqrt{\frac{3}{Y}}\left(\frac{48}{\beta Y}\right)^{1/4}\left(1 - \frac{3\omega}{8Y}\right) \tag{5}$$

$$k = -\frac{27}{5Y}\left(\sqrt{\frac{\beta Y}{48}} - \frac{\beta}{24}\right)\left(1 - \frac{\omega}{12Y}\right) \tag{6}$$

where $\beta = 11 - 2n_f/N_c$. The peak position on each distribution in Fig. 1 can be obtained by fitting (2) to the ξ distribution. The measured peak position for AMY data are plotted in Fig. 3 together with those of low energies from the BES collaboration (in the range of 2.2–4.8 c.m.) [4] and from high energy e^+e^- and ep data [17, 18].

MLLA–LPHD predicts the energy dependence of the peak position, ξ^* as [2]

$$\xi^* = 0.5Y + \sqrt{cY} - c \tag{7}$$

where $c = a^2/16N_cb$, $a = (11N_c/3) + (2n_f/3N_c^2)$, and $b = (11N_c - 2n_f)/3$. By fitting our AMY data to (2), we obtain $\Lambda_{eff} = 263 \pm 8$ MeV. The error quoted in the value is statistical only. This value is consistent with the results from BES [4], OPAL [6], ZEUS [19], and CDF [20], which are 262 ± 9 (e^+e^-), 263 ± 4, 251 ± 14 (ep) and 256 ± 13 ($p\bar{p}$) MeV, respectively. The errors inserted for the other experiments are also statistical only. Figure 3 also shows that ξ^* is approximately

Fig. 3. Energy dependence of the peak position ξ^* for various experiments [4, 17, 18].

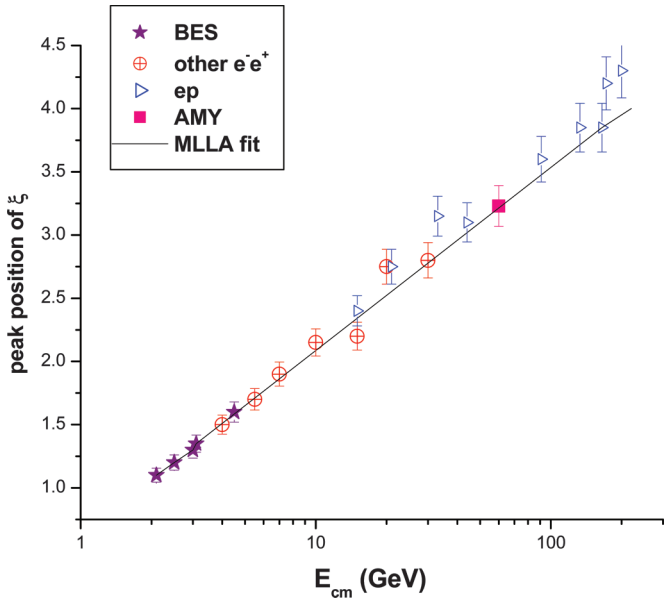

Fig. 4. Invariant density Edn/d^3p of charged particles in e^+e^- annihilation as a function of the particle energy $E = (p^2 + Q_0^2)^{1/2}$ at $Q_0 = 270$ MeV. Data at various c.m. energies are compared to MLLA predictions with the overall normalization adjusted (from ref. 30).

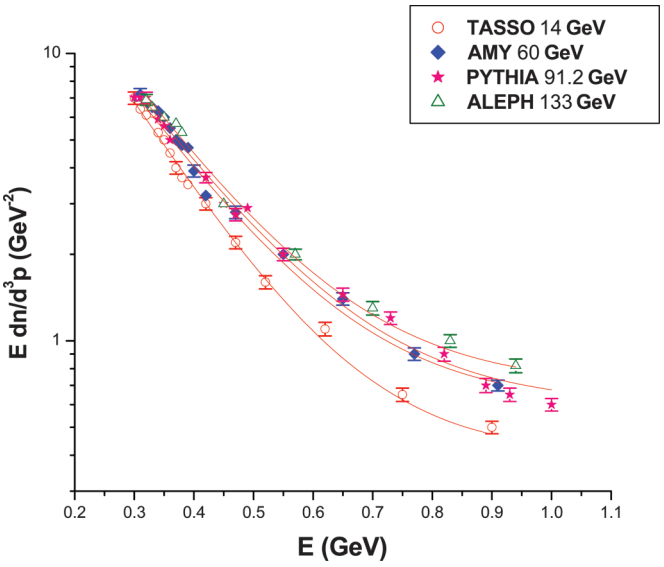

linear in ln $\sqrt{s}$. This behavior is consistent with the prediction of the QCD calculations [6]. A straight line fit of our results (together with the results from other experiments) to ξ^* as a function of $\sqrt{s}$ gives a gradient of 0.0801 ± 0.130. The gradients reported by BES [4], OPAL [21], ZEUS [22], and H1 [23] are 0.779 ± 0.122, 0.0637 ± 0.016, 0.650 ± 0.077, and 0.75 ± 0.05, respectively.

The QCD scale Λ_{eff} is related to the (running) strong coupling constant (single loop) by [24]

$$\frac{\alpha_s}{2\pi} = \frac{1}{bY} = \frac{1}{b\ln(E_{\text{beam}}/\Lambda_{\text{eff}})} \tag{8}$$

A value of α_s extracted from (8) for $N_c = 3$, $n_f = 3$ in our AMY data is α_s (60 GeV) = 0.128 ± 0.04. This value is consistent within the statistical errors with many accurate measurements [25]. We conclude that it is a success of LPHD + MLLA that the extracted value of α_s is correct. However, it is claimed in ref. 24 that this is not a good way to determine α_s accurately, as it is nearly impossible to make a proper estimate of the systematic errors.

It is worth mentioning that the MLLA calculations refer always to one loop calculations. If the number of partons increases, we have to take into account more loops, which indicates that heavier quarks and consequently more flavors are also produced in the interaction. As the MLLA prediction is based on just the leading order, we should consider three flavors only [26–28].

On the other hand, if we use five flavors instead of three in our calculations, the value of the coupling constant obtained is similar to the corresponding value for three flavors within the statistical errors. In addition, the aim of the paper in this section is not to calculate the coupling constant exactly as there are some more accurate methods for calculating the coupling constant up to next-to-next-leading order [29]. The main reason for presenting the coupling constant here is just to show that MLLA prediction works properly, because it gives us the parameter α_s within a range in which the proper α_s is located. Although the systematic error is high, its good approximate value confirms the validity of the MLLA prediction.

4. Momentum spectrum

In Fig. 4 we show the experimental results on the Lorentz invariant density of charged particles Edn/d^3p for AMY data together with those of other experiments up to 130 GeV in e^+e^- annihilation. An approximate energy independence of the soft limit is indeed observed. The same is true for identified particles π, K, and p in the range of 1.6–91 GeV [30]. We conclude that hadron production at very small momentum is approximately energy independent [31]. This behavior has been explained in ref. 22 as the coherent emission of lower energy (i.e., long wavelength) gluons by the total color current.

5. Charged particle multiplicity

We measure the charged particle multiplicity distribution and derive several related quantities from it, in particular, the mean charged multiplicity $\langle n_{\text{ch}}\rangle$ and the second binomial moment $R_2 = \langle n_{\text{ch}}(n_{\text{ch}} - 1)\rangle/\langle n_{\text{ch}}\rangle^2$. Figure 5 shows the mean multiplicity of charged particles measured in e^+e^- annihilation by various experiments [12, 32, 33]. One finds an excellent agreement between the data and the analytical QCD expectations [22].

The second binomial moment is a measure of the strength of hadron–hadron correlations and a sensitive probe for higher order QCD or non-perturbative effects. According to the next leading order (NLO) QCD calculations, R_2 is given by [4],

$$R_2 = \frac{11}{8}[1 - c\sqrt{\alpha_s(\sqrt{s})}] \tag{9}$$

with $c = 0.55$ (0.56) for five (three) active flavors. There has been a long-standing discrepancy between the value of R_2 calculated by NLO and that measured by e^+e^-, μ^+p, and $\nu_\mu p$ experiments [4].

Based on the measured multiplicity distribution, we obtain the second binomial moments R_2, which are displayed in Fig. 6 together with both NLO calculations and published data at higher energies up to 200 GeV from e^+e^- experiments [34]. Our AMY R_2 value, as well as the values obtained from Monte Carlo PYTHIA data, is consistent with other measurements at lower and higher energies. The R_2 value predicted by leading order QCD is significantly higher than the measured data, and while the NLO calculations come closer to data, the

Fig. 5. The mean multiplicity of charged particles measured by e^+e^- annihilation by various experiments [12, 32, 33].

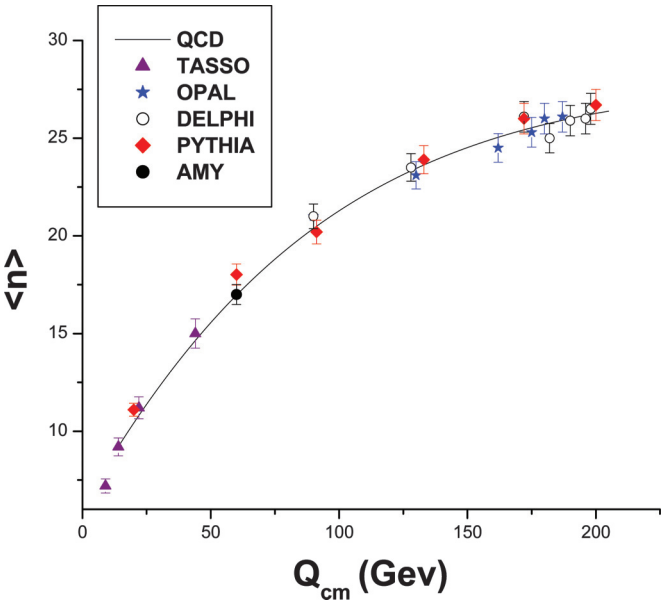

Fig. 6. Energy dependence of the second binomial moment R_2. The QCD results in the leading order, NLO (MLLA) [31] in comparison with experimental data [34].

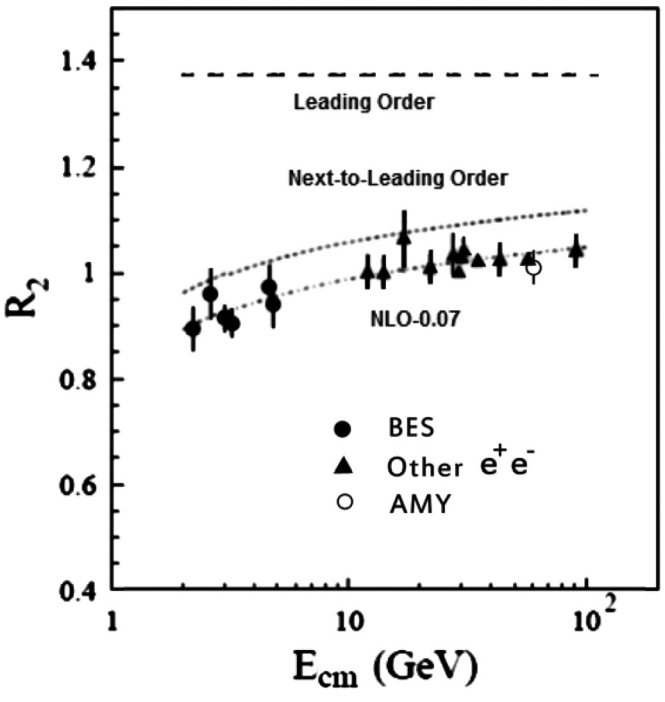

remaining disagreement of about ~0.07 in R_2 may indicate that R_2 is a sensitive probe for higher order QCD or non-perturbative effects [4].

6. Summary and conclusion

We measure in this article the inclusive momentum spectra, multiplicity distributions, and the second binomial moments for both the AMY and the Monte Carlo PYTHIA data. The measured distributions and derived quantities, in combination with corresponding results obtained at lower and higher energies, are compared to QCD Monte Carlo models and to analytical QCD predictions calculated in various approaches.

The LPHD + MLLA approach is an interesting attempt to understand some properties of multi-hadron production in terms of perturbative QCD. This approach tries to take QCD as near as possible to the limits imposed by confinement. It gives predictions for properties of momentum spectra that can be compared with experimental data, but concentrates on observables that can be described without too many unknown free parameters [24].

The experimental values of the parameter ξ for various hadrons and at different c.m. energies indicate the dependence of ξ on the c.m. energy. This can be described adequately by the MLLA calculations. Next, the experimental results on the momentum spectrum for AMY data together with those of other experiments up to 130 GeV in e^+e^- annihilation, show an energy independence of soft limit. This behavior has been explained as the coherent emission of lower energy (i.e., long wavelength) gluons by the total color current [22].

Based on the measured multiplicity distribution, our AMY R_2 value as well as the values from Monte Carlo PYTHIA data are consistent with other measurements at lower and higher energies. The R_2 value predicted by leading order QCD is significantly higher than the measured data, and while the NLO calculations come closer to data, the remaining disagreement of about ~0.07 in R_2 may indicate that R_2 is a sensitive probe for higher order QCD or non-perturbative effects [4]. However, In general, a good agreement is found between the measurements and the corresponding QCD predictions. We have extracted from the QCD scale Λ_{eff} the strong coupling constant with a value of 0.128 ± 0.04. We conclude that it is a success of LPHD + MLLA that the extracted value of α_s is correct within the systematic errors.

References

1. H. Fritzsch, M. Gell-Mann, and H. Leutwyler. Phys. Lett. B, **47**, 365 (1973); D.J. Gross and F. Wilczek. Phys. Rev. D, **8**, 3633 (1973). doi:10.1103/PhysRevD.8.3633; H.D. Politzer. Phys. Rep. **14**, 129 (1074).
2. V.A. Khoze and W. Ochs. Int. J. Mod. Phys. A, **12**, 2949 (1997). doi:10.1142/S0217751X97001638.
3. Ya.I. Azimov, Yu.L. Dokshitzer, V.A. Khoze, and S.I. Troyan Phys. Lett. B, **165** (1985).
4. BES Collaboration, J.Z. Bai, et al. Phys. Rev. D, **69**, 072002 (2004). arXiv:hep-ex0306055v2.
5. Y.K. Li, AMY Collaboration, et al. Phys. Rev. D, **41**, 2675 (1990). doi:10.1103/PhysRevD.41.2675; Y.K. Kim, et al. Phys Rev. Lett. **63**, 1772 (1989). doi:10.1103/PhysRevLett.63.1772.
6. OPAL Collaboration, G. Abbiendi, et al. Eur. Phys. J. C, **16**, 185 (2000). doi:10.1007/s100520050015.
7. ALEPH Collaboration, E. Barate, D. Buskulic, D. Decamp, et al. Phys. Rep. **294**, 1 (1998). doi:10.1016/S0370-1573(97)00045-8.
8. DELPHI Collaboration, P. Aberu, et al. Eur. Phys. J. C, **6**, 19 (1999).
9. L3 Collaboration, B. Adeva, O. Adriani, M. Aguilar-Benitez, et al. Phys. Lett. B, **259**, 199 (1991). doi:10.1016/0370-2693(91)90159-N.
10. MARK II Collaboration, G.S. Abrams, C.E. Adolphsen, D. Averill, et al. Phys. Rev. Lett. **64**, 1334 (1990). doi:10.1103/PhysRevLett.64.1334.
11. ALEPH Collaboration, D. Buskulic, et al. Z. Phys. C, **73**, 409 (1997). doi:10.1007/s002880050330.
12. OPAL Collaboration, R. Akers, et al. Z. Phys. C, **72**, 191 (1996); K. Ackerstaff, et al. Z. Phys. C, **75**, 193 (1997).
13. AMY Collaboration, H.W. Zheng, et al. Phys. Rev. D, **42**, 737 (1990). doi:10.1103/PhysRevD.42.737.
14. DELPHI Collaboration, P. Abreu, W. Adam, T. Adye, et al. Phys. Lett. B, **372** 172 (1996); Ibid. Phys. Lett. B, **416**, 233 (1998). doi:10.1016/S0370-2693(97)01248-3..
15. TASSO Collaboration, W. Braunschweig, et al. Z. Phys. C, **47**, 187 (1990). doi:10.1007/BF01552339.
16. C.P. Fong and B.R. Webber. Nucl. Phys. B, **355**, 54 (1991). doi:10.1016/0550-3213(91)90302-E.
17. M. Schmelling. Phys. Scr. **51**, 683 (1995). doi:10.1088/0031-8949/51/6/004.
18. O. Biebel. Phys. Rep. **340**, 165 (2001). doi:10.1016/S0370-1573(00)00072-7.
19. V.A. Jamieson. Ph. D thesis, DESY F35 D-95-01.
20. A. Safonov. *In* 8th International Work-shop on Deep Inelastic Scattering and QCD (DIS2000). Fermilab-Conf-00-131-EM.
21. OPAL Collaboration, M.Z. Akrawy, G. Alexander, J. Allison, et al. Phys. Lett. B, **247**, 617 (1990). doi:10.1016/0370-2693(90)91911-T.
22. ZEUS Collaboration, M. Derrick, D. Krakauer, S. Magill, et al. Z. Phys. C, **67**, 93 (1995). doi:10.1007/BF01564824.
23. H1 Collaboration, S. Aid, V. Andreev, B. Andrieu, et al. Nucl. Phys. B, **445**, 3 (1995). arXiv: hep-ex/9505003.
24. N.C. Brummer. 1994. arXiv: hep-ex/9405001.

25. J. Schieck. Nucl. Phys. B, **234**, 225 (2013). arXiv: hep-ex/1208.4588v1.
26. W. Ochs and R.P. Ramos. Phys. Rev. D, **78**, 034010 (2008). arXiv:0807.1082v1. doi:10.1103/PhysRevD.78.034010.
27. OPAL Collaboration, G. Abbiendi, et al. Eur. Phys. J. C, **27**, 467 (2003). arXiv: hep-ex/0209048. doi:10.1140/epjc/s2002-01121-3.
28. V. Khoze, S. Lupia, and W. Ochs. Phys. Lett. B, **386**, 451 (1996). arXiv:hep-ph/9604410. doi:10.1016/0370-2693(96)00922-7.
29. OPAL Collaboration, G. Abbiendi, C. Ainsley, P.F. Åkesson, et al. Eur. Phys. J. C, **71**, 1733 (2011). doi:10.1140/epjc/s10052-011-1733-z; L. Khajooee, T. Kalalian, R. Saleh-Moghaddam, A. Sepehri, and M.E. Zomorrodian. Acta Phys. Polon. B, **45**, 1077 (2014). doi:10.5506/APhysPolB.45.1077.
30. V.A. Khoze, S. Lupia, and W. Ochs. Phys. Lett. B, **394**, 179 (1997). doi:10.1016/S0370-2693(96)01668-1.
31. P. Aberu, et al. Phys. Lett. B, **459** 397, (1999).
32. TOPAZ Collaboration, R. Itoh, M. Yamauchi, A. Yamaguchi, et al. Phys. Lett. B, **345**, 335 (1995). doi:10.1016/0370-2693(94)01685-6.
33. DELPHI Collaboration, P. Abreu, et al. Z. Phys. C, **73**, 11 (1996). doi:10.1007/s002880050295; Ibid. Z. Phys. C, **73**, 229 (1997).
34. E.D. Malaza and B.R. Webber. Phys. Lett. B, **149**, 501 (1984); Ibid. Nucl. Phys. B, **267**, 70 (1986). doi:10.1016/0550-3213(86)90138-0.
35. C.P. Fong and B.R. Webber. Phys. Lett. B, **229**, 289 (1989). doi:10.1016/0370-2693(89)91174-X.
36. Yu.L. Dokshitzer, V.S. Fadin, and V.A. Khoze. Phys. Lett. B, **115**, 242 (1982). doi:10.1016/0370-2693(82)90654-2.
37. ALEPH Collaboration, D. Decamp, B. Deschizeaux, C. Goy, et al. Phys. Lett. B, **273**, 181 (1991). doi:10.1016/0370-2693(91)90575-B.